Sensors and Materials, Vol. 38, No. 2 (2026) 629–634
MYU Tokyo

S & M 4331

Radiation-induced Luminescence of Eu-doped Ga_2O_3–SiO_2 Glasses

Akihiro Nishikawa,[1*] Daiki Shiratori,[2] Takumi Kato,[1]
Daisuke Nakauchi,[1] Noriaki Kawaguchi,[1] and Takayuki Yanagida[1]

[1]Nara Institute of Science and Technology, 8916-5 Takayama, Ikoma, Nara 630-0192, Japan
[2]Department of Electrical Engineering, Tokyo University of Science, 6-3-1 Niijuku,
Katsushika-ku, Tokyo 125-8585, Japan

(Received October 21, 2025; accepted December 9, 2025)

Keywords: glasses, scintillator, Eu

In this study, Eu-doped (0.1, 0.3, 1.0, and 3.0%) Ga_2O_3–SiO_2 glasses were synthesized by the melt-quenching method using a floating zone furnace. The 0.1–1.0% Eu samples were partially crystallized glasses, which included the cristobalite phase, whereas the 3.0% Eu sample indicated only a halo pattern. All the samples showed the emission originating from divalent Eu ions at around 450 nm in photoluminescence and scintillation. Therefore, it was found that self-reduction occurred in all the samples. The full-energy peak under irradiation with α-rays of ^{241}Am was observed in all the samples, and the 1.0% Eu sample showed the highest light yield of 100 photons/5.5 MeV.

1. Introduction

The divalent Eu ion shows luminescence in the range of UV to NIR, depending on the host material, and the lifetime is from several hundred ns to several μs.(1,2) The trivalent Eu ion exhibits orange-red luminescence, with a lifetime of several ms.(3,4) Thus, divalent and trivalent Eu ions have been utilized as luminescence centers in phosphors for various applications, including LED,(5,6) long-afterglow phosphors,(7–9) optical thermometry,(10,11) and scintillators.(12–14) Scintillators are one type of phosphor that can emit lower-energy photons when irradiated with ionizing radiation. New scintillators have been actively developed, and the scintillation properties of various materials have been reported.(15–20) SrI_2:Eu and CaF_2:Eu are typical commercial scintillators, which are used for the detection of γ-rays. In addition, LiF:Eu is a commercial scintillator, which is used for the detection of thermal neutrons. The divalent Eu ion serves as the luminescence center in those scintillators. Eu-doped glasses have been studied actively for LED and X-ray imaging applications. There are many studies on trivalent Eu-activated glasses;(21,22) in contrast, studies on divalent Eu-activated glasses are relatively few, since trivalent Eu ions are generally more stable than the divalent state in oxide glasses. Controlling the reduction reaction (Eu^{3+} to Eu^{2+}) in glass is challenging, and many researchers

---

[*]Corresponding author: e-mail: nishikawa.akihiro.nc6@ms.naist.jp

https://doi.org/10.18494/SAM6008

ISSN 0914-4935 © MYU K.K.
https://myukk.org/

have studied it by incorporating halide elements and gas flow to create a reduction atmosphere.(23,24) In addition, the self-reduction reaction of Eu ions in glass under an air atmosphere has been reported.(25,26) Several self-reduction mechanisms have been proposed, including electron donation by electron trap vacancies and non-bridging oxygen, as well as the evaporation of certain elements.(26,27) The photoluminescence (PL) and scintillation properties of the Eu-doped Al_2O_3–SiO_2 glasses were investigated in our previous study,(28) and the glasses exhibited luminescence originating from divalent Eu ions resulting from self-reduction. Consequently, it was found that the glasses had a capacity of detecting α-rays. In this study, we focused on Ga_2O_3–SiO_2 glasses. Ga is of the same group element as Al, and Ga_2O_3 is an intermediate oxide, which is the same as Al_2O_3.(29,30) Thus, it is expected that the glasses will show the luminescence of divalent Eu ions resulting from self-reduction. Therefore, the PL and scintillation properties of Eu-doped Ga_2O_3–SiO_2 glasses were investigated to develop a new optical glass material.

2. Materials and Methods

2.1 Sample preparation

Eu-doped $10Ga_2O_3$–$90SiO_2$ glass ceramics were made by the melt-quenching method using an optical floating zone (FZ) furnace. The starting materials of the host glass, namely, Ga_2O_3 (4N) and SiO_2 (4N) powders, were uniformly mixed. The Eu_2O_3 (4N) powder was added to the host glass at concentrations of 0.1, 0.3, 1.0, and 3.0 mol%. A total of 4 g of these powders was mixed in an agate mortar. The mixed powders were formed into a cylindrical rod using hydrostatic pressure, and this rod was sintered at 1200 °C for 8 h in air. The optical FZ furnace (FZ-T-12000-X-VPO-PC-Y, Crystal Systems) melted the obtained ceramic rod with four Xe lamps. In addition, the molten part was dropped into the water and was rapidly quenched.

2.2 Measurement method

Powder X-ray diffraction patterns were measured using MiniFlex 600 (Rigaku). Diffuse transmittance spectra were measured with a spectrophotometer (SolidSpec-3700, Shimadzu). PL excitation/emission maps and PL quantum yields (QYs) were measured using Quantaurus-QY (C11347, Hamamatsu Photonics). Quantaurus-Tau (C11367, Hamamatsu Photonics) was used to measure PL lifetimes. Scintillation spectra were obtained with our laboratory-made setup.(31) Light yields (LYs) were estimated from pulse height spectra measured using our original setup.(31)

3. Results and Discussion

Figure 1(a) shows the appearance and XRD patterns of all the samples. The 0.1–1.0 Eu samples showed a halo pattern and crystalline peaks. The peaks would originate from the cristobalite phase, based on the reference pattern. However, the ratio of crystalline peak intensity

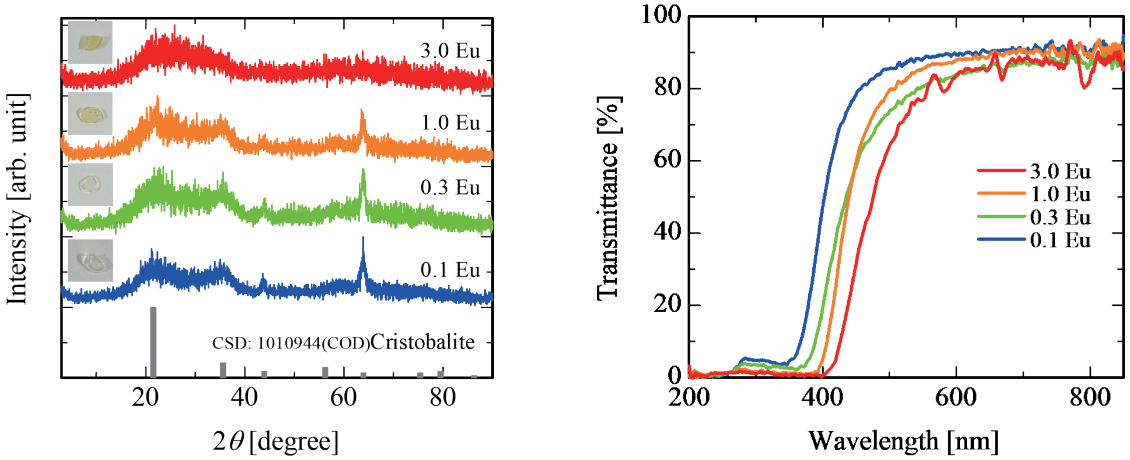

(a) (b)

Fig. 1. (Color online) (a) Appearance and XRD patterns, and (b) diffuse transmittance spectra.

was different from the reference pattern, which suggested the possibility of oriented crystallization.(32,33) On the other hand, the 3.0 Eu sample showed only a halo pattern. Figure 1(b) shows the diffuse transmittance spectra; all the samples showed high transmittance in the visible region. The peaks at approximately 580, 670, and 800 nm in the 3.0 Eu sample were likely due to machine artifacts. The broad absorption at around 350 nm was observed in all the samples and redshifted with increasing Eu concentration. It matched the excitation wavelength of divalent Eu ions, as mentioned below; thus, the absorption was attributed to the 4f-5d transitions of divalent Eu ions.

Figure 2(a) shows the PL emission/excitation map of the 0.3 Eu sample. All the samples indicated the same trend in the PL emission/excitation map. Thus, the result of the 0.3 Eu sample was displayed as a representative. The broad emission at around 400–550 nm was observed in all the samples. To confirm the origin of the emission, decay curves monitored at 450 nm were measured. Figure 2(b) shows the PL decay curves and the lifetimes. Two exponential decay components approximated all the decay curves, and the lifetimes were attributed to the 5d-4f transition of divalent Eu ions.(34,35) Therefore, it was found that the Ga_2O_3–SiO_2 partially crystallized glasses and glass had self-reduction (Eu^{3+} to Eu^{2+}). The lifetimes of the 0.3–3.0 Eu samples decreased with increasing Eu concentration. The QYs of the 0.1–3.0 Eu samples monitored for the emission of the divalent Eu ions were 8, 9, 5, and 2%, respectively. The QYs showed the same trend as lifetimes, which would be due to a concentration quenching effect.

Figure 3(a) shows the X-ray-induced scintillation spectra. The broad emission at around 450 nm and the sharp emissions at around 575, 590, 610, and 645 nm were observed in all the samples. The broad emission would be attributed to the 5d-4f transition of divalent Eu ions,(36,37) the same as PL, and the sharp emissions would be attributed to the 4f-4f transitions ($^5D_0 \rightarrow {}^7F_0$, $^7F_1$, $^7F_2$, and $^7F_3$) of trivalent Eu ions.(38–40) In the PL spectra, the emission of the trivalent Eu ions was not observed, but the emission was clearly observed in scintillation spectra. The difference in the excitation source and the sensitivity of the detector might affect the result. Furthermore, a redshift was observed in the broad emission resulting from self-absorption.

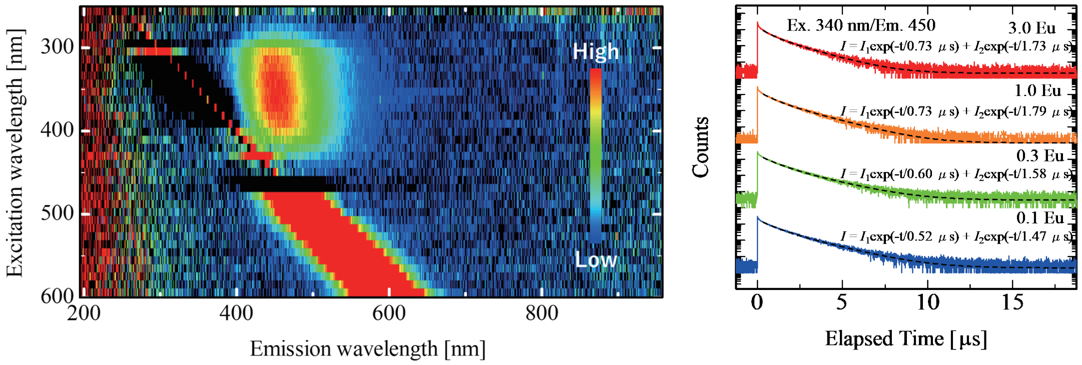

(a) (b)

Fig. 2. (Color online) (a) PL emission/excitation map of the 0.3 Eu sample. (b) PL decay curves.

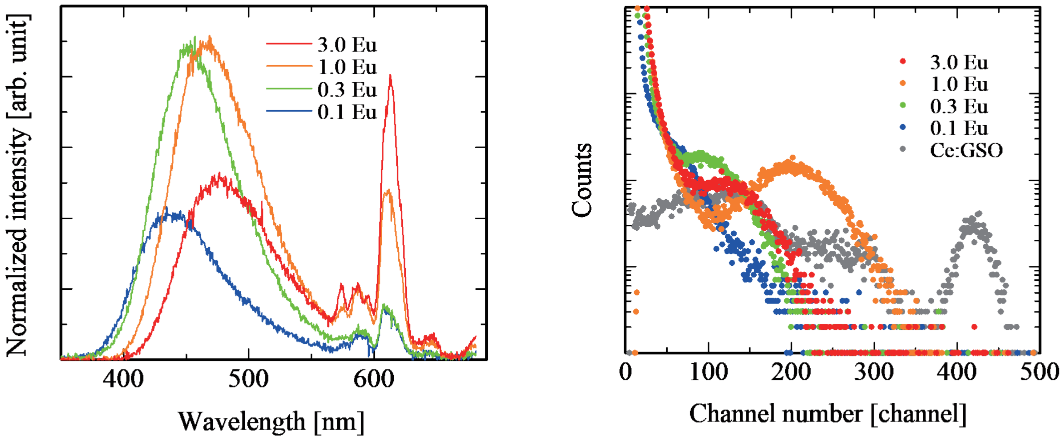

(a) (b)

Fig. 3. (Color online) (a) X-ray-induced scintillation spectra and (b) pulse height spectra.

Figure 3(b) shows the pulse height spectra under ^{241}Am α-ray irradiation. The photoabsorption peak under the γ-ray irradiation of ^{137}Cs of Gd_2SiO_5: Ce (7000 photons/MeV) was used as a reference. LY was calculated using the channel number of the full-energy peak and quantum efficiency (QE). The QE was the emission-weighted quantum efficiency calculated from the scintillation spectra in the range of 270–550 nm. The QEs of the 0.1–3.0 Eu samples and reference sample were 29.75, 28.00, 25.58, 24.06, and 29.58, respectively. The shaping time of all the samples was 2 μs. The calculated LYs of the 0.1–3.0 Eu samples were 15, 40, 100, and 60 photons/5.5MeV, respectively.

4. Conclusion

Eu-doped Ga_2O_3–SiO_2 glasses with Eu concentrations of 0.1, 0.3, 1.0, and 3.0% were prepared by the melt-quenching method using an FZ furnace. From the XRD pattern, the 0.1–1.0 Eu samples had the cristobalite phase, whereas the 3.0 Eu sample did not show the crystalline phase. In the PL and scintillation, the luminescence of the divalent Eu was observed. Thus, it was found that self-reduction occurred in the Ga_2O_3–SiO_2 glass and partially crystallized glasses. The LYs of all the samples were evaluated using α-rays of ^{241}Am, and the highest LY was 100 photons/5.5 MeV. In future work, to apply the scintillator, enhancing LY is necessary.

Acknowledgments

This work was supported by JSPS Fellows (24KJ1699), JSPS KAKENHI (22H00309, 23K25126, 24K03197, and 25K08266), and the Cooperative Research Project of the Research Center for Biomedical Engineering.

References

1 Z. Tang, Q. Zhang, Y. Cao, Y. Li, and Y. Wang: Chem. Eng. J. **388** (2020) 124231. https://doi.org/10.1016/j.cej.2020.124231
2 H. Terraschke and C. Wickleder: Chem. Rev. **115** (2015) 11352. https://doi.org/10.1021/acs.chemrev.5b00223
3 X. Chen, H. Yu, K. Sheng, Y. Zhang, C. Wang, N. Wu, M. Xie, and R. Yu: J. Alloys Compd. **1039** (2025) 183120. https://doi.org/10.1016/j.jallcom.2025.183120
4 J. Zheng, H. Wang, S. Lin, Z. Pan, Q. Yang, and J. Liu: J. Alloys Compd. **1010** (2025) 177668. https://doi.org/10.1016/j.jallcom.2024.177668
5 H. Zhao, X. Yao, X. Tian, L. Guo, S. Cheng, Y. Ran, D. Li, D. Gao, H. He, S.-W. Chen, X. Liu, Y. Yang, and R. Yu: Opt. Mater. (Amst). **159** (2025) 116656. https://doi.org/10.1016/j.optmat.2025.116656
6 X. Yang, Q. Sun, Y. Liu, X. Wang, J. Jing, H. Zou, Y. Song, and Y. Sheng: Ceram. Int. **51** (2025) 1508. https://doi.org/10.1016/j.ceramint.2024.11.123
7 Y. Suda, T. Okuno, Y. Kamigaki, and H. Miyagawa: J. Appl. Phys. **138** (2025) 083107. https://doi.org/10.1063/5.0276657
8 H. Zhang, M. Sun, J. Zhang, Z. Zuo, R. Zhang, J. Duan, and B. Hou: J. Alloys Compd. **1010** (2025) 176711. https://doi.org/10.1016/j.jallcom.2024.176711
9 Y. Wang, M. Shi, B. Yang, J. Ren, Q. Wang, Y. Wang, C. Hu, J. Li, Y. Shi, O. Shichalin, E. Papynov, I. Buravle, and J. Zou: Ceram. Int. **51** (2025) 40735. https://doi.org/10.1016/j.ceramint.2025.05.360
10 Y. Li, J. Song, L. Meng, M. Jiao, Q. Xu, C. Yang, and Z. Xu: J. Alloys Compd. **1010** (2025) 178079. https://doi.org/10.1016/j.jallcom.2024.178079
11 J. Czajka, M. Runowski, C. Hernández-Álvarez, I. R. Martín, and A. Szczeszak: Sci. Rep. **15** (2025) 18950. https://doi.org/10.1038/s41598-025-03683-4
12 H. Fukushima, R. Tsubouchi, T. Matsuura, T. Yoneda, and T. Yanagida: Sensors Mater. **37** (2025) 487. https://doi.org/10.18494/SAM5438
13 S. Muneta, N. Kawano, D. Nakauchi, T. Kato, K. Okazaki, K. Ichiba, T. Kunikata, A. Nishikawa, K. Miyazaki, F. Kagaya, K. Shinozaki, and T. Yanagida: Sensors Mater. **37** (2025) 509. https://doi.org/10.18494/SAM5441
14 D. Nakauchi, T. Kato, N. Kawaguchi, and T. Yanagida: Jpn. J. Appl. Phys. **62** (2023) 010607. https://doi.org/10.35848/1347-4065/ac9181
15 Y. Endo, K. Ichiba, D. Nakauchi, T. Kato, N. Kawaguchi, and T. Yanagida: Sensors Mater. **36** (2024) 473. https://doi.org/10.18494/SAM4758
16 R. Tsubouchi, H. Fukushima, T. Kato, D. Nakauchi, S. Saijo, T. Matsuura, N. Kawaguchi, T. Yoneda, and T. Yanagida: Sensors Mater. **36** (2024) 481. https://doi.org/10.18494/SAM4763
17 K. Miyazaki, D. Nakauchi, T. Kato, N. Kawaguchi, and T. Yanagida: Sensors Mater. **36** (2024) 515. https://doi.org/10.18494/SAM4756
18 T. Kato, D. Nakauchi, N. Kawaguchi, and T. Yanagida: Sensors Mater. **36** (2024) 531. https://doi.org/10.18494/SAM4749
19 M. Koshimizu, K. Tanahashi, Y. Fujimoto, and K. Asai: Sensors Mater. **37** (2025) 539. https://doi.org/10.18494/SAM5448
20 H. Masai and T. Yanagida: Jpn. J. Appl. Phys. **62** (2023) 010606. https://doi.org/10.35848/1347-4065/ac91b8
21 S. Sharma, A. Khanna, M. Milanova, A. Yordanova, R. Iordanova, D. Yang, and B. Chen: J. Lumin. **286** (2025) 121393. https://doi.org/10.1016/j.jlumin.2025.121393
22 Y. D. Narad, Y. R. Parauha, and S. J. Dhoble: J. Non. Cryst. Solids **655** (2025) 123446. https://doi.org/10.1016/j.jnoncrysol.2025.123446

23 S. Batygov, M. Brekhovskikh, L. Moiseeva, I. Zhidkova, and S. Yurtaeva: J. Non. Cryst. Solids **480** (2018) 57. https://doi.org/10.1016/j.jnoncrysol.2017.06.029

24 M. Nogami: J. Phys. Chem. B **119** (2015) 1778. https://doi.org/10.1021/jp511513n

25 H. Chen, C. Zhou, X. Chen, C. Min, S. Lin, Y. Li, T. Zhou, J. Kang, C. Shi, C. Shao, P. Han, W. Strek, H. Chen, and L. Zhang: J. Am. Ceram. Soc. **108** (2025) e20237. https://doi.org/10.1111/jace.20237

26 L. Gan, R. Li, W. Zhong, W. Zhou, L. Yu, and S. Lian: J. Alloys Compd. **1009** (2024) 177043. https://doi.org/10.1016/j.jallcom.2024.177043

27 Q. Zhang, X. Liu, Y. Qiao, B. Qian, G. Dong, J. Ruan, Q. Zhou, J. Qiu, and D. Chen: Opt. Mater. (Amst). **32** (2010) 427. https://doi.org/10.1016/j.optmat.2009.10.002

28 A. Nishikawa, D. Shiratori, S. Rim, T. Kato, D. Nakauchi, N. Kawaguchi, and T. Yanagida: Solid State Sci. **160** (2025) 107812. https://doi.org/10.1016/j.solidstatesciences.2024.107812

29 J. Ren and H. Eckert: J. Phys. Chem. C **118** (2014) 15386. https://doi.org/10.1021/jp504023k

30 L. A. Balewick and J. E. Shelby: J. Am. Ceram. Soc. **72** (1989) 1751. https://doi.org/10.1111/j.1151-2916.1989.tb06320.x

31 T. Yanagida, K. Kamada, Y. Fujimoto, H. Yagi, and T. Yanagitani: Opt. Mater. (Amst). **35** (2013) 2480. https://doi.org/10.1016/j.optmat.2013.07.002

32 L.-Y. Wang and M.-H. Hon: Ceram. Int. **21** (1995) 187. https://doi.org/10.1016/0272-8842(95)90909-3

33 C. Rüssel: J. Non. Cryst. Solids **219** (1997) 212. https://doi.org/10.1016/S0022-3093(97)00271-8

34 Y. Kishimoto, X. Zhang, T. Hayakawa, and M. Nogami: J. Lumin. **129** (2009) 1055. https://doi.org/10.1016/j.jlumin.2009.04.031

35 H. Bouchouicha, G. Panczer, D. de Ligny, Y. Guyot, M. L. Baesso, L. H. C. Andrade, S. M. Lima, and R. Ternane: J. Lumin. **169** (2016) 528. https://doi.org/10.1016/j.jlumin.2014.11.054

36 Y. Isokawa, H. Kimura, T. Kato, N. Kawaguchi, and T. Yanagida: Opt. Mater. (Amst). **90** (2019) 187. https://doi.org/10.1016/j.optmat.2019.02.046

37 A. Herrmann, A. Simon, and C. Rüssel: J. Lumin. **132** (2012) 215. https://doi.org/10.1016/j.jlumin.2011.08.024

38 Z. Lian, J. Wang, Y. Lv, S. Wang, and Q. Su: J. Alloys Compd. **430** (2007) 257. https://doi.org/10.1016/j.jallcom.2006.05.002

39 I. I. Kindrat and B. V. Padlyak: Opt. Mater. (Amst). **77** (2018) 93. https://doi.org/10.1016/j.optmat.2018.01.019

40 C. Nico, R. Fernandes, M. P. F. Graça, M. Elisa, B. A. Sava, R. C. C. Monteiro, L. Rino, and T. Monteiro: J. Lumin. **145** (2014) 582. https://doi.org/10.1016/j.jlumin.2013.08.041